Investigation on the Effect of Impeller Design Parameters on Performance of a Low Specific Speed Centrifugal Pump Using Taguchi Optimization Method

Hadi Ayremlouzadeh[1], Samad Jafarmadar[1,*] and Seyed Reza Amini Niaki[2,*]

[1]*Mechanical Engineering Department, Faculty of Engineering, Urmia University, Urmia, Iran*
[2]*Japan Agency for Marine-Earth Science and Technology; 3173-25 Showa-machi, Kanazawa-ku, Yokohama 236-0001, Japan*
E-mail: s.jafarmadar@urmia.ac.ir; r.amini@jamstec.go.jp
[*]*Corresponding Author*

Received 17 September 2021; Accepted 08 November 2021;
Publication 07 January 2022

Abstract

In order to investigate the effect of blade design on pump performance, a CFD analysis was carried out, and the results were compared with experimental performance data of a low specific speed radial pump, which presents a good agreement. After model verification, the effect of impeller geometrical parameters includes blade outlet angle, wrap angle, and width at the exit, was investigated on the pump's performance. Moreover, these parameters were chosen on three levels using an L9 orthogonal standard array of the Taguchi optimization method. The efficient levels of variables were calculated using the analysis of variance (ANOVA) method. The results revealed that impeller width at exit and blade outlet angle is the most effective pump shaft power and efficiency parameters. To minimize power, the optimal levels are the outlet

International Journal of Fluid Power, Vol. 23_2, 161–182.
doi: 10.13052/ijfp1439-9776.2322

angle of 27°, wrap angle of 150°, and width at the exit of 9 mm. Further, an outlet angle of 23°, a wrap angle of 155°, and a width at the exit of 9 mm lead to maximum pump efficiency. According to the validation simulations, an increase of 2.4% inefficiency and a minimum power of 3.9KW were achieved. The Overall Evaluation Criteria (OEC) technique revealed that considering 23°, 160°, and 9 mm for outlet angle, wrap angle, and width at the exit, minimum shaft power, and maximum pump efficiency will be achieved. ANOVA introduced width at the exit as the most governing parameter of pump performance characteristics.

Keywords: Centrifugal pump, Taguchi optimization method, numerical simulation, blade design parameters, ANOVA.

1 Introduction

The centrifugal pump's function is to transport multiple types of fluids by converting rotational energy from the impeller to the hydrodynamic energy of the flow [1]. To meet all demands of different industries, there is an increase in trend towards improving pump efficiency with stricter manufacturing limitations [2]. They involve many variables in the centrifugal pump impeller design parameters, which influence the overall pump performance, such as blade outlet angle, wrap angle, and width at the exit [3]. Evaluating these factors and setting up the corresponding values leads to new problems and a greater need to find innovative approaches [4]. Considerable effort has already been invested in studying the centrifugal pump and turbomachines performance [5–8]. Therefore, flow characteristics in centrifugal pumps have been the subject of numerous investigations [9, 10]. There are various methods to optimize the pump design and manufacturing. With improved computational fluid dynamic software, analysis of flow and pump performance based on numerical simulation is one of the strategic tools [11, 12]. Experimental and theoretical studies have been done to improve the low specific speed centrifugal pump efficiency since 1970. These pumps are a type of centrifugal pump with a specific speed (Ns) of 0 to 25 and are widely used in oil and gas refineries, petrochemicals, marine industries, and so on. Impeller design is a critical factor in Centrifugal pump performance. Efficiency depends on blade geometrical parameters such as blade number, thickness, wrap angle, inlet, outlet angle, etc., which have attracted many researchers' attention.

The effect of the blade number on a centrifugal pump performance was investigated by Houlin et al. [13]. They selected four different blade numbers with a fixed volute design and the same geometrical parameters of the impeller. The outcome confirmed that the pump head increases to a specific optimized level with an increase in blade number and then decreases. In another work, the effect of blade numbers on a centrifugal pump performance was examined by Chakraborty et al. [14]. Their results revealed that the impeller with ten blades has the highest head. However, the frictional loss and although hydraulic loss increases due to the interface between fluid flow and blades for higher blade numbers. Moreover, with an increment of blade number, velocity increases, which causes impeller casting problems [15–17].

The flow pattern inside the impeller is affected mainly through blade inlet, outlet, and wrap angles. For example, longer flow passage and consequently increase in friction losses result from higher wrap angle. In contrast, a small flow passage leads to poor control of the flow in the impeller. The effect of blade wrap angle on pump performance was studied by [18]. They reported that the pump with a large wrap angle has preferable efficiency and proper operation. In another work, due to the importance of blade outlet angle, a radial impeller with three different outlet angles of 20°, 30°, and 50° was investigated by [19]. They found that rising the outlet blade angle yields a smoother and flatter performance curve.

According to the [20] results, hydraulic performance for a low specific speed pump improves due to the larger blade outlet angle. The performance of high specific speed pumps with different blade outlet angles of 23, 25, 27, 29, and 31° was numerically investigated [20]. Their founding revealed that, especially in high flow rates, the effect of blade outlet angle on efficiency is more noticeable. In this case, the hydraulic loss of the impeller becomes larger at a higher blade outlet angle. Based on the importance of impeller inlet geometry, Lou et al. [21] showed that a large inlet angle has a preferred influence on improving cavitation in a pump. The effect of four inlet blade angles, including 20, 27, 35, 45, and 60°, was investigated by Yousefi et al. [22]. They reported that a centrifugal pump with a 45° inlet angle has the highest performance, the most uniform velocity distribution around the blade, and a steady flow in the inlet zone. Design of experiments (DOE) is a systematic approach to understanding how process and product parameters affect response characteristics. Some of the researches on the application of different DOE tools on pump performance and impeller design can be found in [23–26], which uses optimization methods such as response

surface method (RSM), genetic algorithm (GA), artificial bee colony (ABC) algorithm, etc.

As a DOE method, the Taguchi [27, 28] design is a proper experimental method to optimize the response variable, using fewer experiments than a factorial design. This method in industries aims to make a powerful and easy-to-use experimental design and apply this to product development cycle time for both design and production, therefore decreasing costs and increasing profit. Although impeller design parameters have been investigated in different researches and various optimization methods, have been utilized, but there is no study on pump performance optimization by the Taguchi method. Therefore, in the present study, the geometrical parameters of a low specific speed ship water pump impeller, which is used for cooling the ship motor, were calculated manually using the Lobanoff method [29]. The pump was assembled and experimentally tested in an industrial laboratory, and then the results of performance characteristics were compared with numerical results. Since experimentally studying all parameters is expensive, after verifying the simulated model, the Taguchi method was carried out to optimize the impeller design factors affecting the pump's performance characteristics. Also, an analysis of variance (ANOVA) and overall Evaluation Criteria (OEC) were done to see the contribution percentage of each parameter and the effective parameter levels to gain the best performance of the pump.

2 Experimental Work

2.1 Hydraulic Design

The first step of pump design is a hydraulic design of impeller and volute. Manual calculation based on the Lobanoff method was utilized with the input data of 33 m^3/h flow rate, 31 m head, and 2980 rpm of rotational speed. The liquid was 18°C water with a density of 999 kg/m^3, and the direction of rotation was clockwise. *Ns* of the pump is calculated as following and is a dimensionless number:

$$N_s = \frac{N \times Q^{0.5}}{H^{0.75}} \tag{1}$$

where *N* is rotational speed in rpm, *Q* is pump flow rate in m^3/s and *H* is pump head in m. This equation leads to N_s of 21.72 which puts the pump in low specific speed pump region. Lobanoff method leads to calculating of number of blades, impeller inlet and outlet diameters, width at exit, inlet and outlet angles, blade profile and volute parameters which are presented in Table 1.

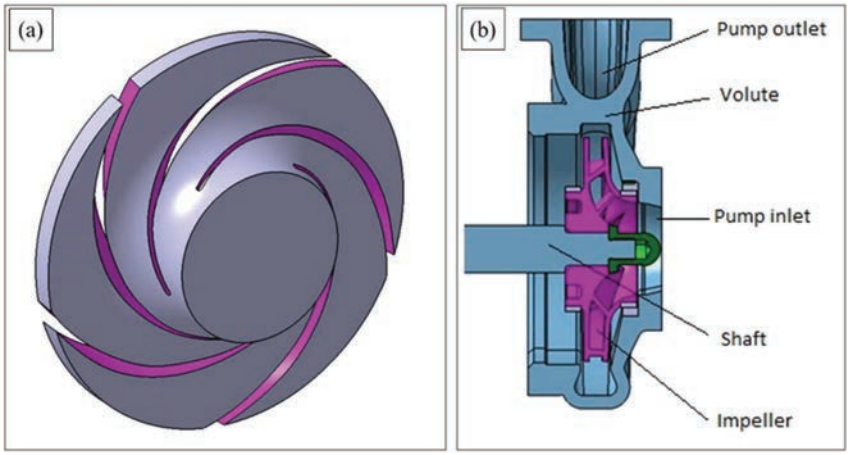

Figure 1 (a) Hydraulic profile of impeller and (b) Assembled model of centrifugal pump.

Table 1 Pump geometric characteristics

Characteristics	Value
Impeller inlet diameter – D_1 (mm)	72
Impeller outlet diameter – D_2 (mm)	162
Blade inlet angle – β_1 (°)	40
Blade outlet angle – β_2 (°)	25
Blade wrap angle – ω (°)	155
Impeller width at exit – b_2 (mm)	10
Blade thickness – e (mm)	4∼6
Number of blades – N	5
Volute suction diameter – D_{Suc} (mm)	63.5
Volute discharge diameter – D_{dis} (mm)	50

2.2 Mechanical Design

Figure 1(a) presents the hydraulic profile of the impeller designed by a CAD code. THE 3D CAD model of pump parts was also prepared in real dimension (not scaled), which is illustrated in Figure 1(b). Table 1 has listed volute geometric characteristics. Moreover, designed impeller casting model and manufactured impelled illustrated in Figure 2(a) and 2(b), respectively.

2.3 Performance Test

The experimental performance test setup schematic of the pump is presented in Figure 3. Performance test of the pump was carried out for around 30 min

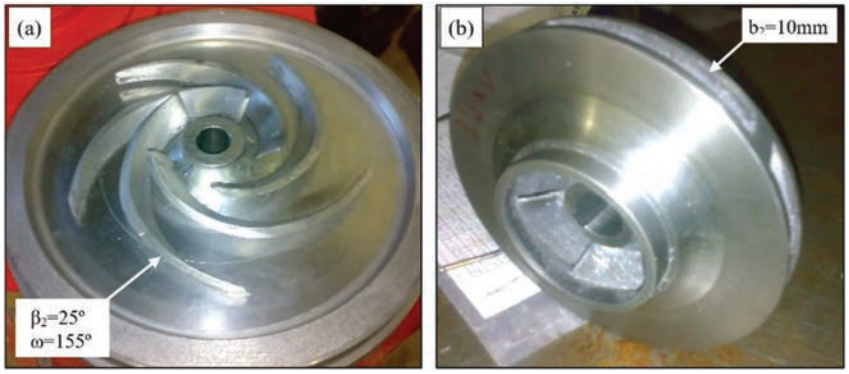

Figure 2 (a) Pump impeller casting model and (b) Manufactured impeller.

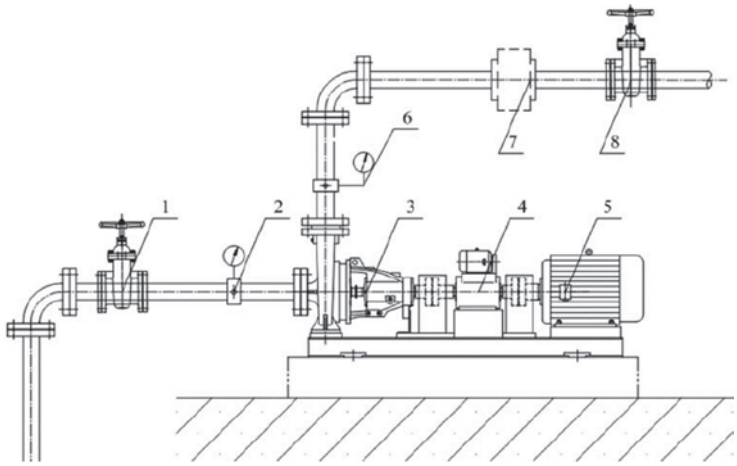

Figure 3 Schematic diagram of centrifugal pump performance test apparatus: 1. inlet valve; 2. vacuum gauge; 3. centrifugal pump; 4. torque meter; 5. motor; 6. pressure gauge; 7. flow meter; and 8. outlet valve (Tan et al., 2012).

and the data of ΔP (pressure difference between discharge and suction) and input power were measured. Pump efficiency is calculated as the following:

$$\eta_{pump} = \frac{\rho g Q H}{P} \tag{2}$$

where ρ is fluid density, g is gravitational constant, Q is capacity, H is pump head acquired from ΔP and P is pump power and which is calculated as:

$$P = \sqrt{3} V I \cos(\varphi) \eta_{EM} \tag{3}$$

Where V, I, $\cos(\varphi)$, and η_{EM} are voltage, amperage measured by a flow meter, power factor determined in electromotor datasheet by manufacturer, and electromotor efficiency.

3 Simulation

Simulation is an efficient way to explore a whole process or system. The act of simulating something first requires that a model be developed. The model represents the system itself, whereas the simulation represents the operation of the system over time [30]. Schematic of computational domains meshing can be observed in Figure 4.

The Navier–Stokes momentum, continuity, and turbulence equations using a finite volume method were solved. Since the flowing fluid is turbulence, a realizable k-e turbulence model was selected. The governing equations for k and ε are as follows:

$$\frac{\partial}{\partial \mathrm{t}}(\rho \mathrm{k}) + \frac{\partial}{\partial \mathrm{x_i}}(\rho \mathrm{k u_i}) = \frac{\partial}{\partial \mathrm{x_j}}\left[\left(\mu + \frac{\mu_\mathrm{t}}{\sigma_\mathrm{k}}\right)\frac{\partial \mathrm{k}}{\partial \mathrm{x_j}}\right] + \mathrm{G_k} + \mathrm{G_b} - \rho\varepsilon - \mathrm{Y_M} + \mathrm{S_k} \tag{4}$$

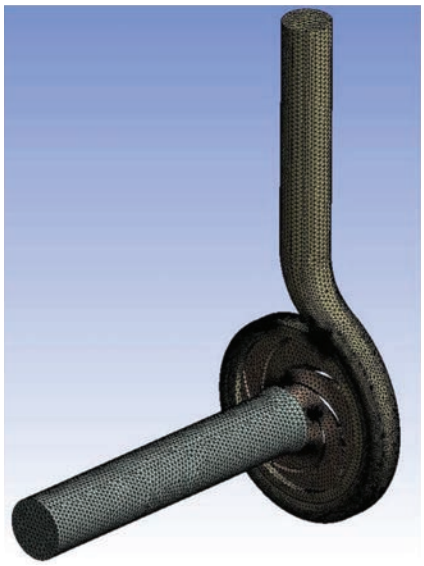

Figure 4 Computational grid on flow inside the pump.

$$\frac{\partial}{\partial \mathrm{t}}(\rho\varepsilon)+\frac{\partial}{\partial \mathrm{x_i}}(\rho\varepsilon \mathrm{u_i})=\frac{\partial}{\partial \mathrm{x_j}}\left[\left(\mu+\frac{\mu_\mathrm{t}}{\sigma_\varepsilon}\right)\frac{\partial\varepsilon}{\partial \mathrm{x_j}}\right]$$
$$+\mathrm{C_1}\frac{\varepsilon}{\mathrm{k}}(\mathrm{G_k}+\mathrm{G_{3\varepsilon}G_b})-\mathrm{C_{2\varepsilon}}\frac{\varepsilon^2}{\mathrm{k}}+\mathrm{S}_\varepsilon \tag{5}$$

And,

$$\mathrm{C_1}=\max\left[0.43\ \&\frac{\eta}{\eta+5}\right] \tag{6}$$

$$\eta=\mathrm{S}\frac{\mathrm{k}}{\varepsilon} \tag{7}$$

$$\mathrm{S}=\sqrt{2\mathrm{S_y}} \tag{8}$$

where G_k represents the generation of turbulence kinetic energy due to the mean velocity gradients, G_b is the generation of turbulence kinetic energy due to buoyancy, Y_M represents the contribution of the fluctuating dilatation in compressible turbulence to the overall dissipation rate, C_2 and $C_{1\varepsilon}$ are constants. σ_k and σ_ε are the turbulent Prandtl numbers for k and ε, respectively. S_k and S_ε are user-defined source terms. In this research, the computational domain consists of 4 zones: inlet, outlet, impeller, and volute. Since the impeller is a rotational part, whereas other domains stay stationary, the multi-reference frame (MRF) technique was established. The impeller is placed in a rotating reference frame and volute in the fixed reference frame. Mass conservation and momentum equation in MRF technique are as:

$$\frac{\partial\rho}{\partial t}+\nabla\cdot\rho\vec{\nu}_r=0 \tag{9}$$

$$\frac{\partial(\rho\vec{\nu}_r)}{\partial t}+\nabla\cdot(\rho\vec{\nu}_r\vec{\nu})+\rho(\vec{\omega}\times\vec{\nu})=-\nabla P+\nabla\cdot t+\vec{F} \tag{10}$$

$$\frac{\partial(\rho E)}{\partial t}+\nabla\cdot(\rho\vec{\nu}_r H+\rho\vec{u}_r)=\nabla\cdot(\mathrm{k}\nabla\mathrm{T}) \tag{11}$$

where $\vec{\nu}_r$ is relative speed, $\vec{\nu}$ is absolute speed and $\vec{u}_r$ is rotational speed [31].

An inlet pressure boundary condition and a mass flow inlet boundary condition with a mass flow rate of 9.16 kg/s were set at the inlet and outlet surface of the fluid domain, respectively.

In the MRF technique, the impeller was selected as a moving frame with a constant rotational speed of 2980 rpm, and inlet, outlet, and volute speeds, as the stationary frames, were set to zero. Water with a density of 998.2 kg/m^3 and viscosity of 0.001 kg/m.s was selected as the working fluid.

Table 2 Selected levels of impeller design

Variable	Level 1	Level 2	Level 3
Blade outlet angle (β_2) ($^\circ$)	23	25	27
Blade wrap angle (ω) ($^\circ$)	150	155	160
Blade width at exit (b_2) (mm)	9	9.5	10

3.1 Taguchi Experimental Design

Previous investigations showed that impeller design parameters are among the most effective parameters on the performance characteristics of a centrifugal pump. Based on these studies and after the comparison of experimental and numerical results and verification of the simulated model, three control factors, including blade outlet angle ($\beta 2$), blade wrap angle (ω), and blade width at exit (b2), were selected and presented in Table 2.

Using the full factorial method would require $3^3 = 27$ experiments, while an L9 orthogonal array, as presented in Table 3, drastically reduced the number of required experiments to nine. To scan the effect of changing a particular parameter on a process or product, a signal-to-noise ratio (S/N) is a simple quality indicator. A larger S/N ratio means smaller noise, which yields to better final results. Depending upon what the objective of quality characteristic is, there are two major S/N ratio types. In order to maximize the response, the following S/N is used:

$$\mathrm{S/N} = -10 \log_{10} \left[\frac{1}{\mathrm{n}} \sum_{\mathrm{i}=0}^{\mathrm{n}} \frac{1}{\mathrm{x_i^2}} \right] \tag{12}$$

and when minimizing the response is favorable, the S/N ratio can be calculated as:

$$\mathrm{S/N} = -10 \log_{10} \left[\frac{1}{\mathrm{n}} \sum_{\mathrm{i}=0}^{\mathrm{n}} \mathrm{x_i^2} \right] \tag{13}$$

$\mathrm{x_i}$ is the value of the response, and n is the number of repeats [32]. Since the optimum levels for each individual response may differ, an Overall Evaluation Criterion (OEC) method is utilized to obtain the best conditions where all responses are in their optimum values. Based on the significance of each response, a relative weight is attributed in the range of 0–100%, and the following equation calculates the OEC value:

$$\mathrm{OEC} = \frac{\mathrm{X_1}}{\mathrm{X_{1ref}}} \times \mathrm{Wt_1} + \frac{\mathrm{X_2}}{\mathrm{X_{2ref}}} \times \mathrm{Wt_2} + \cdots \tag{14}$$

Table 3 Designed L9 orthogonal standard array

Exp.	β_2 (°)	ω (°)	b2 (mm)	Model Code
1	1	1	1	$\beta_2$23, ω150, $b_2$9
2	1	2	2	$\beta_2$23, ω155, $b_2$9.5
3	1	3	3	$\beta_2$23, ω160, $b_2$10
4	2	1	2	$\beta_2$25, ω150, $b_2$9.5
5	2	2	3	$\beta_2$25, ω155, $b_2$10
6	2	3	1	$\beta_2$25, ω160, $b_2$9
7	3	1	3	$\beta_2$27, ω150, $b_2$10
8	3	2	1	$\beta_2$27, ω155, $b_2$9
9	3	3	2	$\beta_2$27, ω160, $b_2$9.5

Where X1 is the evaluated value under criterion 1 and X1ref is the highest value of X1, and Wt1 is the relative weight of criterion 1 [27]. The sum of the weights necessarily should be 100. Analysis of variance (ANOVA) is a statistical method to estimate the relative contribution of each control factor on response. In this research, ANOVA of S/N data has been investigated to reduce the variation on outputs.

4 Results and Discussion

4.1 Experimental and Numerical Results Comparison

A radial flow ship water pump with data presented in Table 1 was designed, manufactured, and tested in an industrial laboratory. The experimental test results of flow rates corresponding to about 0 (shut off point), 14.1, 24.4, 33.1 (rated flow), 40, 44.6, and 54.9 (end of the curve) all in m^3/h, were compared with simulation ones. Figures 5–7 demonstrate the comparison of experimental and theoretical results for pump head, power, and efficiency, respectively. Frictional, hydraulic, and mechanical loss is responsible for the almost lower experimental head and efficiency curve comparing to numerical ones. It is evident that numerical and experimental results of head and efficiency for different flow rates are in a satisfactory correlation even in high flow rates. A lower volumetric flow rate of the fluid will have a lower velocity in which the diameter of the pipe remains unchanged (suction and discharge side). A lower velocity will cause a lower pipe pressure drop and fitting pressure drop. Therefore, the head of a pump decreases also, since the head is calculated as $\frac{\Delta P}{\rho g} + \frac{\Delta V^2}{2g}$.

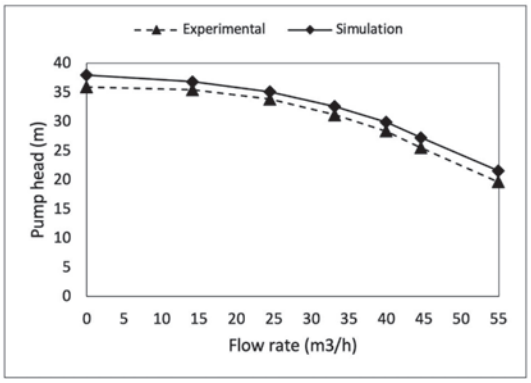

Figure 5 Experimental and numerical results comparison for pump head.

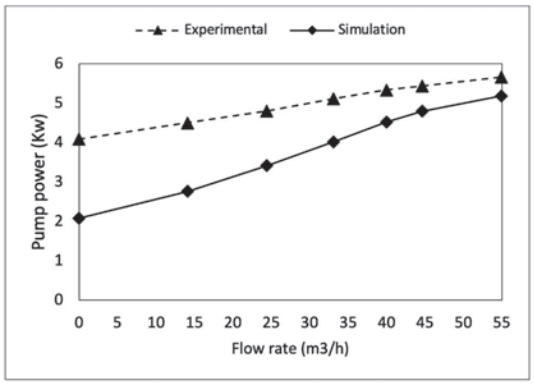

Figure 6 Experimental and numerical results comparison for pump power.

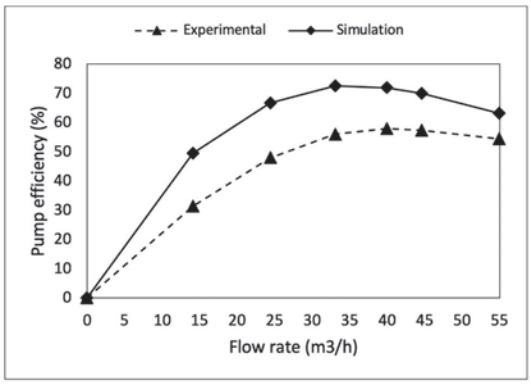

Figure 7 Experimental and numerical results comparison for pump efficiency.

4.2 Contours of Static Pressure and Velocity

Figure 8 shows static pressure contour for different designs in the impeller and centrifugal pump. As this Figure reveals, the pressure increases gradually along with the impeller and has higher pressure on the pressure side than the suction side for each design. Pressure rises along with the discharge, confirms the correct impeller rotating direction. The velocity contour of each design for the impeller can be observed in Figure 9. Here is visible that the velocity increases as the fluid moves towards the discharge of the impeller.

4.3 S/N Ratio

The data of head, power, and efficiency besides S/N ratio results are listed in Table 4, considering the smaller, the better response for pump power and the larger, the better response for pump efficiency.

The S/N ratio response plots of the pump head, power, and efficiency are shown in Figure 10. The highest S/N ratio for each factor provides optimal process conditions, which correspond to impeller outlet angle of 23°, impeller wrap angle of 150° and width at the exit of 9 mm for pump head, impeller outlet angle of 27°, impeller wrap angle of 150° and width at the exit of 9 mm for pump power and impeller outlet angle of 23°, impeller wrap angle of 155° and width at the exit of 9 mm for pump efficiency. Since optimum levels of power and efficiency are not included in the L9 orthogonal array, two evaluation simulations were performed according to the optimum levels, and the results of pump power and efficiency are listed in Table 5. As can be seen in Figure 10(c), increasing the outlet angle decreases the pump efficiency is rated flow [3, 19]. An increase in outlet angle decreases the pump head (Figure 10(a)) and increases the power (Figure 10(b)). Since outlet angle variation is higher on the pump head (refer to ANOVA results), the efficiency will decrease as the outlet angle increases. An increase in wrap angle leads to a more extended flow passage between the blades and a significant enlargement of friction loss. Therefore, pump head and power will decrease. This reduction is from 150° to 155° noticeable, and in higher wrap angles is almost unchanged. For efficiency, there is an optimum wrap angle. Efficiency increases as the wrap angle increases from 150° to 155° and decreases by increasing from 155° to 160°. For better understanding, interactions of factors on each parameter shall be studied carefully. There is an optimal width (b2) for the impeller where the supreme performance is obtainable.

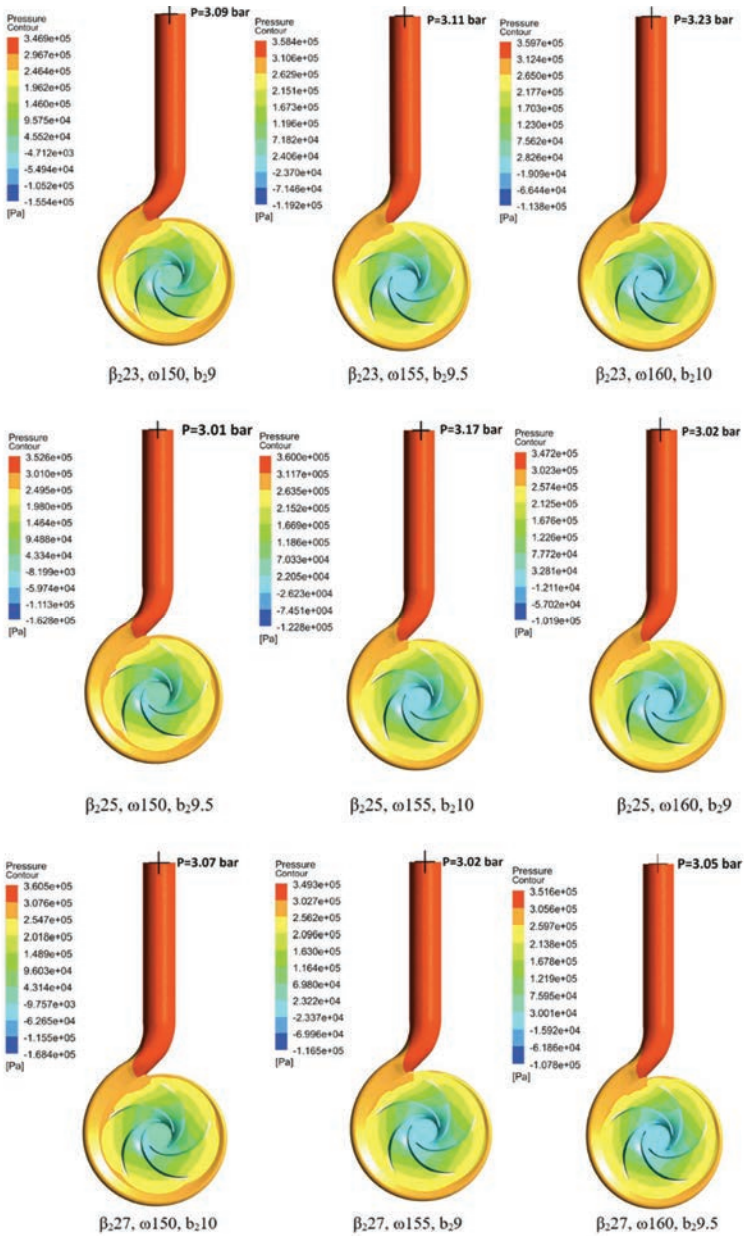

Figure 8 Static pressure contour in impeller and pump discharge for different impeller design (Max. pressure at center of discharge has been mentioned on each counter).

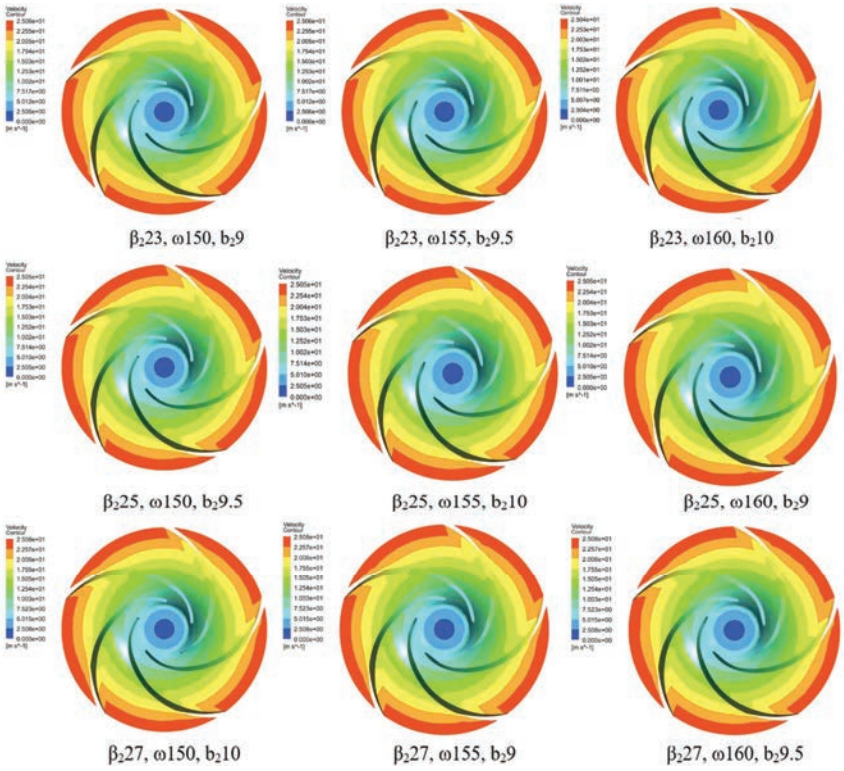

Figure 9 Velocity contour in impeller for different impeller design.

Table 4 Data of pump head, power and efficiency as well as S/N Ratios and OEC results

Model Code	Head (m)	Power (KW)	Efficiency (%)	S/N Ratio of Head	S/N Ratio of Power	S/N Ratio of Efficiency	OEC Results
$\beta_2$23, ω150, $b_2$9	31.62	3.90	72.76	29.9992	−29.99	37.24	83.22
$\beta_2$23, ω155, $b_2$9.5	31.83	3.96	72.08	30.0567	−30.06	37.16	51.66
$\beta_2$23, ω160, $b_2$10	33.05	3.99	72.27	30.3834	−30.38	37.18	64
$\beta_2$25, ω150, $b_2$9.5	30.80	3.96	69.77	29.7710	−29.77	36.89	26
$\beta_2$25, ω155, $b_2$10	32.44	4.02	72.33	30.2216	−30.22	37.19	28.44
$\beta_2$25, ω160, $b_2$9	30.91	3.9	71.12	29.8020	−29.80	37.04	65
$\beta_2$27, ω150, $b_2$10	31.42	4.02	70.05	29.9441	−29.94	36.91	3.11
$\beta_2$27, ω155, $b_2$9	30.91	3.9	71.12	29.8020	−29.80	37.04	65
$\beta_2$27, ω160, $b_2$9.5	31.21	3.96	70.69	29.8859	−29.89	36.99	39.22

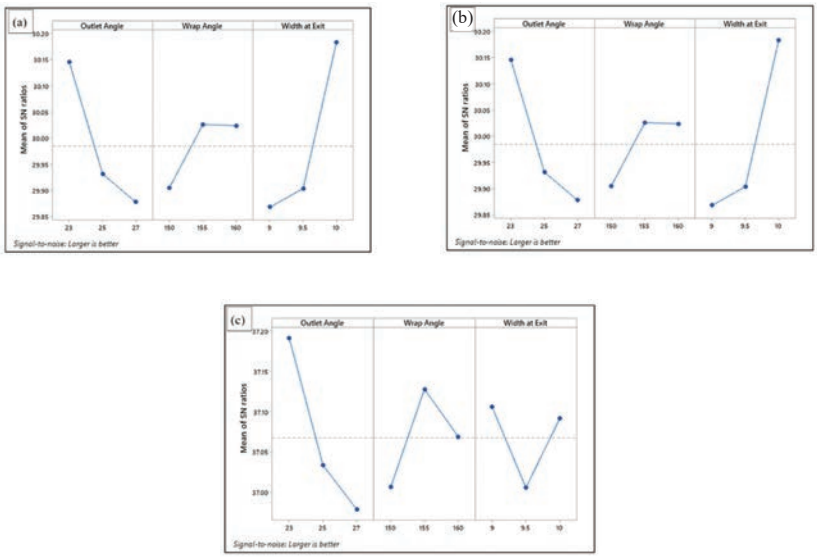

Figure 10 S/N response plot of a) pump head and b) pump power and c) pump efficiency.

Table 5 Simulation results for optimum levels of factors

	Optimum Level of Factors			Simulation Output	
Objective Function	β_2 (°)	ω (°)	b_2 (mm)	Power (KW)	Efficiency (%)
Maximum efficiency	23	155	9	3.96	**74.55**
Minimum power	27	150	9	**3.9**	72.98
OEC	23	160	9	3.9	74.16

4.4 ANOVA Results of Pump Efficiency and Power

The ANOVA was applied to determine the significance of each parameter in the research. The ANOVA results for pump head, power, and efficiency are given in Tables 6–8, respectively. According to the variables' contribution percentage, for the pump head, the most influential parameter is outlet angle, and width at the exit and wrap angle are in the next steps. Also, for pump power, width at exit most affects the response, with a contribution percentage of 51.86%. Results also show that the outlet angle and wrap angle affect the power of the pump. At last, for pump efficiency, the outlet angle was found to be the most influential parameter, with a 95% confidence, followed by a wrap angle and width at the exit.

Table 6 ANOVA result of pump head

	Variable	DOF	Seq. SS	Adj. SS	Adj. MS	Contribution Percentage (%)
1	Blade outlet angle (β_2) (°)	2	12.712	12.712	6.356	48.14
2	Blade wrap angle (ω) (°)	2	2.832	2.832	1.416	10.73
3	Blade width at exit (b_2) (mm)	2	3.541	3.541	1.771	13.41
5	Error	2	7.320	7.320	3.660	27.72
6	Total	8	26.406			100.00

Table 7 ANOVA result of pump power

	Variable	DOF	Seq. SS	Adj. SS	Adj. MS	Contribution Percentage (%)
1	Blade outlet angle (β_2) (°)	2	1.6285	1.6285	0.8142	35.15
2	Blade wrap angle (ω) (°)	2	0.3961	0.3961	0.1980	8.55
3	Blade width at exit (b_2) (mm)	2	2.4029	2.4029	1.2014	51.86
5	Error	2	0.2058	0.2058	0.1029	4.44
6	Total	8	4.6332			100.00

Table 8 ANOVA result of pump efficiency

	Variable	DOF	Seq. SS	Adj. SS	Adj. MS	Contribution Percentage (%)
1	Blade outlet angle (β_2) (°)	2	4.949	4.949	2.4747	54.66
2	Blade wrap angle (ω) (°)	2	1.451	1.451	0.7253	16.02
3	Blade width at exit (b_2) (mm)	2	1.181	1.181	0.5903	13.04
5	Error	2	1.475	1.475	0.7374	16.29
6	Total	8	9.055			100.00

4.5 Overall Evaluation Criterion Results

As it was mentioned, due to the occurrence of different optimum conditions for each objective function, the Overall Evaluation Criteria (OEC) method is suggested to achieve a unique condition. Pump efficiency with the quality characteristic of larger the better and power with the quality characteristic of smaller the better were chosen as OEC responses. Considering the same weight for both objective functions (50% relative weight for each response), the OEC results were calculated and illustrated in Table 4. Figure 11 presents the main effect plots for the S/N ratio of OEC results. These plots indicate that with considering impeller outlet angle of 23°, impeller wrap angle of 160°, and width at the exit of 9 mm, maximum pump efficiency and minimum power will be achieved. A CFD simulation was performed based

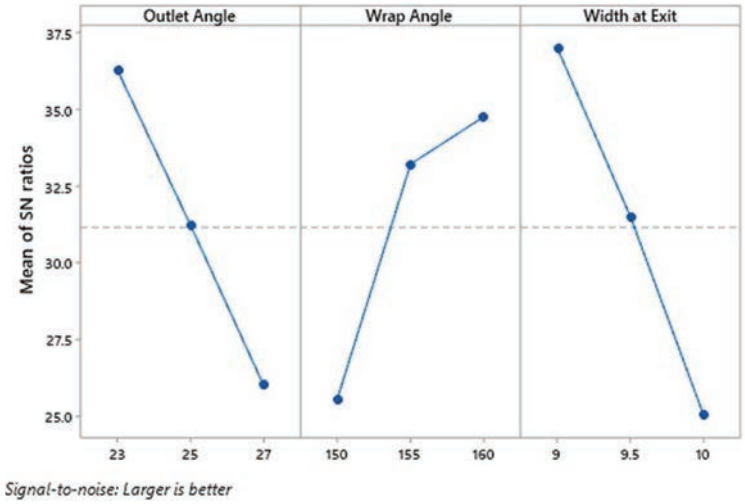

Figure 11 S/N main effect plot of OEC results.

Table 9 ANOVA results of OEC of S/N ratio

	Variable	DOF	Seq. SS	Adj. SS	Adj. MS	Contribution Percentage (%)
1	blade outlet angle (β_2) (°)	2	1648.8	1648.8	824.4	32.70%
2	blade wrap angle (ω) (°)	2	525.8	525.8	262.9	10.43%
3	blade width at exit (b_2) (mm)	2	2620.3	2620.3	1310.1	51.97%
5	Error	2	247.3	247.3	123.7	4.91%
6	Total	8	5042.2	1648.8	824.4	100.00%

on these parametric designs, and the pump head was calculated as 32.13 m, which revealed an efficiency of 74.16% and power of 3.9 KW. These results can be observed in Table 5. As ANOVA results (Table 9) show, efficient parameters are blade width at the exit, blade outlet angle, and blade wrap angle, respectively.

5 Conclusion

How to improve the performance of the pump by changing its geometric characteristics is always challenging. In the present study, an application of a design of experiments (DOE) method in a computational fluid dynamic (CFD) presents to investigate the effect of blade design on pump performance. In this research, the low specific speed radial flow pump was

manufactured and tested. Then the performance of the pump was analyzed using a CFD code, and the results were compared with the experimental ones. After verifying the simulated model, Taguchi's experimental design was carried out to optimize the impeller design parameters affecting the pump's performance characteristics. These parameters include blade outlet angle, blade wrap angle, and blade width at the exit in 3 levels, leading to an L9 orthogonal array. Based on S/N main effect plots for lowest pump power, impeller geometric characteristics, outlet angle, wrap angle, and width at the exit were chosen 27°, 150°, and 9 mm respectively. Moreover, the highest pump efficiency will be achieved with an outlet angle of 23°, a wrap angle of 155°, and a width at the exit of 9 mm. Evaluating simulation revealed 3.9 KW power and 74.55% efficiency for each set, respectively. The analysis of variance (ANOVA) method was considered for statistical analysis and indicated that the outlet angle and width at exit are overcoming efficiency and power, respectively. According to the OEC results, to obtain the lowest power (3.9 KW) and the highest efficiency (74.16%), optimum levels for three factors, including outlet angle, wrap angle, and width at the exit, should be 23°, 160°, and 9 mm, respectively. ANOVA results of OEC data introduced width at the exit as the most governing parameter to affect pump performance characteristics.

References

[1] Nursen EC, Ayder E. Numerical calculation of the three-dimensional swirling flow inside the centrifugal pump volutes. Int J Rotating Mach. 2003;9(4):247–53.
[2] Gopalakrishnan S. Pump research and development: past, present, and future—an American perspective. 1999;
[3] Ding H, Li Z, Gong X, Li M. The influence of blade outlet angle on the performance of centrifugal pump with high specific speed. Vacuum. 2019;159:239–46.
[4] Pei J, Wang W, Yuan S, Zhang J. Optimization on the impeller of a low-specific-speed centrifugal pump for hydraulic performance improvement. Chinese J Mech Eng. 2016;29(5):992–1002.
[5] Acosta AJ. An experimental and theoretical investigation of two-dimensional centrifugal pump impellers. 1952;
[6] Acosta AJ, Bowerman RD. An experimental study of centrifugal pump impellers. 1955.

[7] Howard JHG, Kittmer CW. Measured passage velocities in a radial impeller with shrouded and unshrouded configurations. 1975.
[8] Mouallem J, Mouallem J, Niaki SRA. Picard–Newton iterative algorithm to solve the potential flow equation for different turbomachinery flow regimes. J Brazilian Soc Mech Sci Eng. 2019;41(8):1–10.
[9] Dauherty RL. A further investigation of performance of centrifugal pumps when pumping oils. Bulletin. 1926;130.
[10] Flack RD, Miner SM, Beaudoin RJ. Turbulence measurements in a centrifugal pump with a synchronously orbiting impeller. 1992.
[11] Walther B, Nadarajah S. Constrained adjoint-based aerodynamic shape optimization of a single-stage transonic compressor. J Turbomach. 2013;135(2).
[12] Alemi H, Nourbakhsh SA, Raisee M, Najafi AF. Effect of the volute tongue profile on the performance of a low specific speed centrifugal pump. Proc Inst Mech Eng Part A J Power Energy. 2015;229(2):210–20.
[13] Houlin L, Yong W, Shouqi Y, Minggao T, Kai W. Effects of blade number on characteristics of centrifugal pumps. Chinese J Mech Eng Ed. 2010;6:742.
[14] Chakraborty S, Pandey KM, Roy B. Numerical analysis on effects of blade number variations on performance of centrifugal pumps with various rotational speeds. Int J Curr Eng Technol. 2012;2(1):143–52.
[15] Chakraborty S, Pandey KM. Numerical Studies on Effects of Blade Number Variationson Performance of Centrifugal Pumps at 4000 RPM. Int J Eng Technol. 2011;3(4):410.
[16] Jafarzadeh B, Hajari A, Alishahi MM, Akbari MH. The flow simulation of a low-specific-speed high-speed centrifugal pump. Appl Math Model. 2011;35(1):242–9.
[17] Elyamin GRHA, Bassily MA, Khalil KY, Gomaa MS. Effect of impeller blades number on the performance of a centrifugal pump. Alexandria Eng J. 2019;58(1):39–48.
[18] Tan L, Zhu B, Cao S, Bing H, Wang Y. Influence of blade wrap angle on centrifugal pump performance by numerical and experimental study. Chinese J Mech Eng. 2014;27(1):171–7.
[19] Bacharoudis EC, Filios AE, Mentzos MD, Margaris DP. Parametric study of a centrifugal pump impeller by varying the outlet blade angle. Open Mech Eng J. 2008;2(1).
[20] Cui B, Wang C, Zhu Z, Jin Y. Influence of blade outlet angle on performance of low-specific-speed centrifugal pump. J Therm Sci. 2013;22(2):117–22.

[21] Luo X, Zhang Y, Peng J, Xu H, Yu W. Impeller inlet geometry effect on performance improvement for centrifugal pumps. J Mech Sci Technol. 2008;22(10):1971–6.
[22] Yousefi H, Noorollahi Y, Tahani M, Fahimi R, Saremian S. Numerical simulation for obtaining optimal impeller's blade parameters of a centrifugal pump for high-viscosity fluid pumping. Sustain Energy Technol Assessments. 2019;34:16–26.
[23] Wahba W, Tourlidakis A. A genetic algorithm applied to the design of blade profiles for centrifugal pump impellers. In: 15th AIAA computational fluid dynamics conference. 2001. p. 2582.
[24] Frazier OH, Khalil HA, Benkowski RJ, Cohn WE. Optimization of axial-pump pressure sensitivity for a continuous-flow total artificial heart. J Hear Lung Transplant. 2010;29(6):687–91.
[25] Kim JH, Oh KT, Pyun KB, Kim CK, Choi YS, Yoon JY. Design optimization of a centrifugal pump impeller and volute using computational fluid dynamics IOP Conf. Ser Earth Environ Sci. 2012;15:32025.
[26] Derakhshan S, Pourmahdavi M, Abdolahnejad E, Reihani A, Ojaghi A. Numerical shape optimization of a centrifugal pump impeller using artificial bee colony algorithm. Comput Fluids. 2013;81:145–51.
[27] Roy RK. Design of experiments using the Taguchi approach: 16 steps to product and process improvement. John Wiley & Sons; 2001.
[28] Rao RS, Kumar CG, Prakasham RS, Hobbs PJ. The Taguchi methodology as a statistical tool for biotechnological applications: a critical appraisal. Biotechnol J Healthc Nutr Technol. 2008;3(4):510–23.
[29] Lobanoff VS, Ross RR. Centrifugal pumps: design and application. Elsevier; 2013.
[30] Shojaeefard MH, Tahani M, Ehghaghi MB, Fallahian MA, Beglari M. Numerical study of the effects of some geometric characteristics of a centrifugal pump impeller that pumps a viscous fluid. Comput Fluids. 2012;60:61–70.
[31] Ayremlouzadeh H, Ghafouri J. Computational fluid dynamics simulation and experimental validation of hydraulic performance of a vertical suspended api pump (research note). Int J Eng. 2016;29(11):1612–9.
[32] Phadke MS. Quality engineering using robust design. Prentice Hall PTR; 1995.

Biographies

Hadi Ayremlouzadeh received his M.Sc degree in Mechanical Engineering-Energy Conversion from Tabriz Azad University, Iran, in 2015. He is currently pursuing a Ph.D. degree in Mechanical Engineering-Energy Conversion with the Mechanical Engineering Department of Urmia University, Iran. He had been operating as a mechanical pump designer in the R&D department of PETCO (Iran's largest oil pump manufacturer) for over 12 years. He is now assigned as Pump Hydraulic Laboratory manager in PETCO.

Samad Jafarmadar received his Ph.D. in Internal Combustion Engine from the Tabriz University, Iran, in 2006. He has more than 16 years of teaching, research, and administrative experience. Currently, he is working as a Full-time Professor in the Department of Engineering, Urmia University. His broad research areas include internal combustion engine modeling and exergy analysis in the combustion process and experimental and numerical simulation in heat exchangers. He has published more than 300 research papers in international and national journals/conferences.

Seyed Reza Amini Niaki received his Ph.D. degree in Mechanical Engineering, Fluid and Thermal from the University of Sao Paulo (USP), Brazil, in 2018. My primary research field is CFD modeling and analysis of the multiphase flow. He is currently a Computational Fluid Dynamics Project Research Scientist in the Japan Agency for Marine-Earth Science and Technology (JAMSTEC).